Bull. Chem. Soc. Ethiop. **2010**, 24(3), 361-373. ISSN 1011-3924
Printed in Ethiopia

# MASS CONCENTRATIONS AND ELEMENTAL COMPOSITION OF URBAN ATMOSPHERIC AEROSOLS IN ADDIS ABABA, ETHIOPIA

G. Gebre[1], Z. Feleke[2*] and E. Sahle-Demissie[3]

[1]Environmental Science Program, Addis Ababa University, P. O. Box 1176, Addis Ababa, Ethiopia
[2]Department of Chemistry, Addis Ababa University, P. O. Box 1176, Addis Ababa, Ethiopia
[3]Office of Research and Development, National Risk Management Research Laboratory, OH 45268, USA

(Received December 13, 2009; revised June 4, 2010)

**ABSTRACT**. Aerosol samples were collected from 22 February 2008 to 15 April 2008 and 17 June 2008 to 23 July 2008 in urban and peri-urban areas of Addis Ababa, Ethiopia, with the aim to assess the spatial and temporal aspects of total suspended particulate (TSP) and particulate matter with aerodynamic diameter less than 10 µm ($PM_{10}$) and their composition in terms of metallic elements. Sixty six filter samples were collected from seven distinct sites using I.O.M. multi fraction dust samplers and fiber glass filter papers. The mass of each particulate matter sample was measured gravimetrically and the composition of $PM_{10}$ samples was analyzed using ICP-OAES and SEM-EDAX. The concentration of TSP was in the range of 17-556 $\mu g/m^3$ and that of $PM_{10}$ was in the range of 17-285 $\mu g/m^3$. The highest TSP and $PM_{10}$ peak values were observed in February 2008 at two sites, whereas the lowest TSP and $PM_{10}$ values were observed in June and July 2008 at two sites. The mean TSP concentration surpassed the WHO safe guideline value of 150 $\mu g/m^3$ and 79 % of the $PM_{10}$ values were below the WHO guideline value. The $PM_{10}$ to TSP mass ratio was in the range 0.26-0.59 and $PM_{10}$ mass contributed about 39% to the TSP mass. The average element concentration in $PM_{10}$ filter sample was in the order of Ca > Na > K > Zn > Sb > B > Al > V > Mg > S > Fe. All the analyzed elements contributed about 0.1% to the $PM_{10}$ mass. SEM-EDAX analysis of $PM_{10}$ samples showed that Si, Al, Na, Zn, Ba, K and C were the predominant species. Crustal materials contributed 76-95% of the filter mass, and C and Cu represented 5-24%. The size distribution of aerosol particles as derived from SEM analysis was in 0.43-9.3 µm range.

**KEY WORDS**: TSP, $PM_{10}$, Metal analysis, Atmospheric aerosol, Addis Ababa, Ethiopia

## INTRODUCTION

Addis Ababa is the capital city of Ethiopia and it is a fast-growing urban area in which air quality is affected mainly by increased vehicle emissions, traffic road dust, industrial developments, construction activities, and overall land use practices. Air quality has become a serious concern due to geographical and climatic condition of the city and high air pollutant emissions in the area [1]. There is growing concern for public health, although detailed toxicological and epidemiological studies are non-existent.

The city has a population of more than 2.7 million with a growth rate of 3.8 % [2]. The main rainy season extends from mid June to early September and the dry season extends from October to early June. The small rains, which are short lived and less intense are experienced in March and April. Based on this seasonality, air pollution is likely worst between October and February, when precipitation is minimal and high-pressure systems can cause stagnation episodes [1]. In Ethiopia, limited measurement of air pollutants is available [1]. However, air quality study in Addis Ababa provides only a snapshot of particulate pollutants in dry season (in January/February of 2004) and focused on the major streets. Overall, there is limited information on gaseous pollutants which is mainly focused on ambient CO level [1, 3].

---

*Corresponding author. E-mail: zewge@chem.aau.edu.et ; fbeshah@yahoo.com

Considerable air pollution occurs in large cities throughout the world [4]. It has great impact on the local environment (e.g. on biosphere, buildings and materials) and visibility, and can even influence the surrounding rural areas. The pollution also affects many people inasmuch as these urban areas usually accommodate a large number of inhabitants. The coincidence of the concentrated pollution sources, dense population and/or some times unfavorable geographical and climatic conditions may multiply its adverse effects in particular. Although air pollution and smog problems are very complex, a small set of compounds has been identified as major contributors to the phenomenon. They are called criteria pollutants, and serve as indicators of the air quality in pollution control policy. The criteria pollutants usually include NO and $NO_2$, $SO_2$, CO, tropospheric $O_3$, total or size-fractionated suspended airborne particulate matter [5]. Research into the criteria pollutants and their synergism has revealed that it is the elevated levels of airborne particles that are mainly responsible for the increased health risks of inhabitants in large cities [5-7]

Particulate matter of aerodynamic diameter less than 10 μm, and especially that less than 2.5 μm, has been found to be associated with urban health problems [8]. Many epidemiological studies show that atmospheric aerosols may produce adverse health effects, with recent studies revealing that coarser atmospheric particles are more related to respiratory diseases, whereas the finest particles seem to affect the cardio-vascular system [9-12]. Atmospheric aerosols, especially the sub micrometer-sized particles, also affect the Earth's climate both directly through scattering and absorption of solar radiation and indirectly by acting as cloud condensation nuclei, CCN [13].

Particulate matter pollution arises both from natural and anthropogenic sources. Although the dominant origin of atmospheric aerosols on a global scale is natural [13], in urban areas the main source of atmospheric PM is road traffic [14-16], with diesel vehicles in particular being associated with higher emissions of fine and ultrafine particles [14, 17, 18], exceeding up to 10–100 times those from gasoline vehicles in terms of mass, and up to 105 times in terms of number concentration [17].

Recently in the developed world (Europe and North America) the concentration of particulate matter (PM) has been decreasing due to modern technology employed for pollution prevention and control. However, in some developing countries, such as China and India, the PM concentration has been on the rise due to energy-intensive activities and a similar problem may be expected in African cities. With regard to data on PM and its composition in Africa, extensive work has been done on biomass burning smoke, mainly from savanna fires during dry season campaign [19].

The atmospheric aerosols can be characterized from a number of viewpoints, i.e. by number or mass concentration, chemical composition (elemental, organic and ionic), speciation, size distribution, morphology of the particles and by their source types. Many of these properties are, moreover, interdependent. In addition, the characteristics may display a pronounced variability in time and space due to the wide variety in formation, dynamic transformation, transportation and removal processes of the aerosols. The situation is particularly complicated in highly polluted (urban) air sheds.

In the past 20 years, the composition and sources of $PM_{10}$ aerosols in various environments have been studied in a number of papers [20]. Considerable concerns have arisen on the extent of the pollution, particularly by the presence of metals in airborne particles. These observations lead to investigation of their origin with the development of characterization or speciation studies, using, for example, particle-induced X-ray emission (PIXE) [21], spectroscopy and X-ray fluorescence [22], chemical analysis, and scanning electron microscopy coupled to an energy-dispersive X-ray spectrometer (SEM-EDAX) [23]. Highly sensitive and non-destructive techniques are useful for the direct analysis of particles collected on filters.

The aim of this study is to assess the spatial and temporal aspects of TSP and $PM_{10}$ with emphasis on metal characterization by using ICP-OAES and SEM-EDAX. Electron microscopy may provide valuable information on the morphology, composition, sources, and transformations of atmospheric aerosols. Mass concentration of TSP and $PM_{10}$ in ambient air was also measured for the wet and dry seasons. The result of this study will be useful to understand the status of ambient air quality in Addis Ababa and also provide some information that would be useful for further investigation.

## EXPERIMENTAL

### *Sampling sites*

This research was conducted between 22 February 2008 and 15 April 2008 (for the dry season), and 17 June 2008 to 23 July 2008 (for the wet season). Sampling sites were selected to represent typical and important ambient air quality situations in Addis Ababa (Table 1).

Table 1 Description of sampling sites

| Sample site | Sample code | *Geographical location of sampling points |
|---|---|---|
| Department of Nefas Silk Lafto Police | NSLP | 37 P 0473000; UTM 0991000 |
| Kolfe Keraniyo Custom Check | KoKCC | 37 P 0464338; UTM 0991481 |
| Kotebe Waste Water Treatment | KWWT | 37 P 0483063; UTM 0991418 |
| Kaliti Substation | KSUB | 37 P 0473000; UTM 0981000 |
| Aste T/Giorgis Elementary & Junior School | ATSE | 37 P 0473000; UTM1,001,000 |
| Addis Ababa Stadium | STAD | 37 P 0473072; UTM 0996070 |
| COMESA Leather Technology Institute | COLTI | 37 P 0472704; UTM 0981962 |

*Data in column 3 represents linear distance of X (37 P 0473000) and Y (UTM 0991000) coordinates of the sampling points. 37 P (zone) is a code where a country is located and UTM - Universal Transfer Maker which is a term for satellite navigation system.

Seven distinct sites were selected for ambient aerosols sampling. The sites were chosen systematically so that they represent different socio-economic practices in the urban and peri-urban areas that influence ambient air quality of Addis Ababa (Figure 1). Consequently, topographic map of the city was used to identify the sites taking in to consideration of both geographic distance and land use practices. The sampling sites are located between 5 and 10 km from the geographic center of Addis Ababa which is Nefas Silk Lafto Sub-City Police Department (NSLP). The sampling points within 5 km distance are associated with high socio-economic activities (urban environment) and those points at 10 km distance (peri-urban area) have relatively low level of human interventions.

The identified sampling sites include Nefas Silk Lafto Sub-City Police Department (NSLP), Kolfe Keraniyo Custom Check Point (KoKCC), Kotebe Waste Water Treatment Plant (KWWT), Kaliti Substation (KSUB), Atse T/Giorgis Elementary and Junior School (ATSE), Addis Ababa Stadium (STAD) and COMESA Leather Technology Institute (COLTI). Detailed description of the sampling sites is given below.

Nefas Silk Lafto Sub-City Police Department (NSLP) is located at the geographic centre of Addis Ababa locally known as “Gotera”. It is surrounded by vehicle repair shops, residential houses, commercial firms, fuel depot, Addis Ababa cement factory and Moha Nefas Silk Soft Drinks Factory. Gotera road complex has been under construction while the samples were collected, and the crossroad is one of the most congested traffic areas in the metropolitan.

Kolfe Keraniyo Custom and Security Check Point (KoKCC) is located in the south western part of the city. It is situated in a less congested residential neighborhood that was surrounded by different urban activities. The major land use activities around the site are Kolfe Keraniyo

Custom Check Point, a camp for Federal Police Force, a kindergarten, residential houses, a dairy farm and a wooded area covered by few eucalyptus trees.

Kotebe Waste Water Treatment Plant site (KWWT) is located in the eastern part of Addis Ababa which is found in Bole Sub-City. The major land uses around the site include: a waste water treatment plant, quarries (construction material mining and crushing activities) and very small agricultural practices and an asphalt road (that connects Yerer with CMC and Akaki sub-city) was under construction. The wastewater treatment plant occupied an area of 13.7 hectares which is practices sludge oxidation on a drying bed.

Kaliti substation site (KSUB) is one of Ethiopian Electric Power Corporation (EEPCO) substation which is located in the southern part of the city. The major land use around the site is an agricultural land, and a small village. A mountain peak is located on the western part of the site. This site is considered as a background site.

ATSE site is located in the northern part of Addis Ababa. The land use that is surrounding the sampling site include Atse T/Giorgis Junior and Secondary School, less congested residential houses, a cemetery, a waste water transfer station and a vegetation cover at the upper part.

STAD site is located at the central part of Addis Ababa. The site is surrounded by various forms of socio economic activities including commercial, recreational, service delivery, and high traffic flow. The site is one of the major public attraction (or popular) spots in the city.

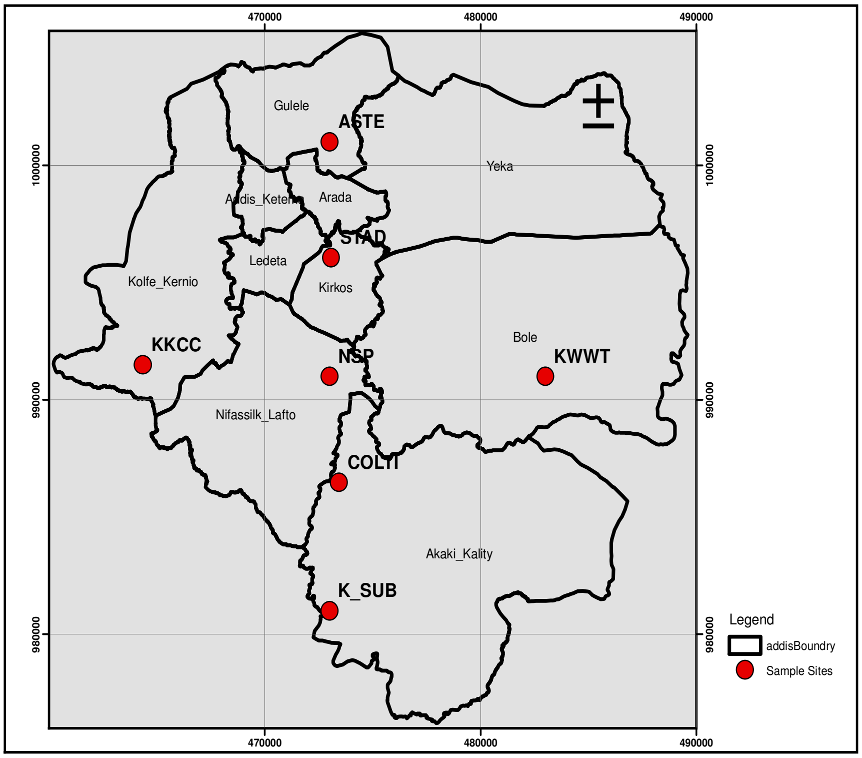

Figure 1. Map showing the TSP and $PM_{10}$ sampling sites.

COLTI sampling site is located in the southern part of Addis. The site was designated as an industrial zone in the revised master plan of Addis Ababa. Consequently, the major land use practice of the site is dominated by manufacturing and processing industries. These include soap, metal works, paint, tanneries, concrete block manufacturing, coffee bean preparation, construction activities, a corrugated iron manufacturing industry and road construction materials processing which are some to be mentioned. Sample from this site was collected inside COMESA Leather Technology Institute compound.

### *Sampling methods*

The sampling unit comprised of portable Institute of Occupational Medicine (IOM) multi fraction dust samplers (made from conductive plastic), tygon hose pipes, battery-operated Universal Air Sampling Pump (SKC 224-PCTX4 Model, SKC Ltd, UK). The samplers were placed at 1.75 m above ground level (Figure 2). The particulate sample collection system was equipped with a vacuum pump, an internal flow regulator, a timer and air flow calibration unit. Air flow calibration was carried out prior to the commencement of sampling and during the course of sampling. Air flow rate was adjusted to 2.0 liters per minute for TSP and 2.2 liters per minute for the $PM_{10}$ as recommended by the manufacturer.

Figure 2. Sampling set up for TSP (left) and $PM_{10}$ (right).

Samples were collected continuously for 24 h. A total of sixty six $PM_{10}$ and TSP samples were collected for analysis. Of these, thirty eight were for the dry season, and twenty eight were for wet season. Each filter paper was oven dried, weighed and stored in desiccator before and after sampling until analysis. The filter papers (Whatman$^{®}$, Whatman International Ltd, Maidstone, England) were placed in static-free plastic cassettes for safe transportation. The cassette was fixed inside the samplers, and then after sampling was complete, the unit was removed and preserved for further analysis.

### *Analytical methods*

The mass of each PM sample was measured gravimetrically. The filters were oven dried at 95±5 $^{o}$C for 2.5 h and weighed prior to and at the end of each sample collection. $PM_{10}$ and TSP filters were collected on a fiber glass filters with 25 mm diameters. The filter samples were weighed using analytical balance with 0.001 mg sensitivity (AT 250, Mettler-Toledo, USA).

Blank filters were transported to and from the measurement site together with the exposed samples and were placed into the sampler over the collection period, to allow equilibrium between the filter medium and the ambient air. These filters were used as blanks to be subtracted from identical filters that were used for particulate sampling.

$PM_{10}$ samples were analyzed in National Risk Management Research Laboratory US EPA, Office of Research and Development Cincinnati, USA. ICP-AES was used to analyze crustal and trace metals found in the filter mass while SEM-EDAX was used to determine the size distribution and composition of particulate matter.

Selected $PM_{10}$ and blank filter samples were analyzed for elements using standard method recommended by USEPA. Inductively Coupled Argon Plasma (ICP) Trace Analyzer Emission Spectroscopy (Optima 3000 Perkin-Elmer Corporation, Nerwalk, Connecticut 06859-0010) was used for elements speciation following acid extraction of filter samples. The samples were extracted in plastic vials using 10 mL of 4% nitric acid and were sonicated for 3 h. The acid solutions were decanted from the filter samples and analyzed using ICP. Filter blanks levels for all elements were negligible as compared with the levels in the PM samples.

Filter samples were further examined to determine the chemical composition of inorganic crystalline particulate matter using scanning electron microscope SEM JOEL-6490LV coupled with Oxford X-Act EDS system. The instrument allowed observation of particles down to 3.5 nm level. In general, 20 and 30 keV beam was applied on the particles to get the image of particulate samples.

## RESULTS AND DISCUSSION

### *Mass concentration*

Figure 3 shows temporal and Figure 4 shows spatial variation of TSP and $PM_{10}$ at the sampling sites, respectively. As can be seen, the weight of particulate matter varied significantly during different sampling period for the same site. The mean TSP mass concentration for the overall sampling duration was 195±141 $\mu g/m^3$. The peak value was 556 $\mu g/m^3$ (February 2008 at NSLP site) and the lowest mass concentration was 17 $\mu g/m^3$ (June 2008 at Kaliti sub-station). It was also noted that the mean TSP concentrations of dry and wet season were 304±102 $\mu g/m^3$ and 75±5 $\mu g/m^3$, respectively.

High TSP value may be attributed to the release of aerosols from road construction, paved and unpaved roads around the sampling site. It can be seen that TSP mass concentration declined starting from the end of March 2008 which is the beginning of rain during this particular year. This indicates the significance of scavenging of atmospheric aerosols by rain.

The mean mass concentration of $PM_{10}$ was 80±61 $\mu g/m^3$. The highest peak value was 285 $\mu g/m^3$ (observed in March 2008 at KWWT site) and the lowest value was 17 $\mu g/m^3$ (observed in July 2008 at COLTI site). The mean $PM_{10}$ mass for dry season was 107±68 $\mu g/m^3$ and that of wet season was 43±21 $\mu g/m^3$. High value for dry season may be attributed to the emission of dust particles from paved and unpaved road and incomplete products of fossil fuel combustion, biomass and waste burning activities around the sampling site. Low $PM_{10}$ value for wet season may be due to scavenging by rain and low level of dust emissions from the paved and unpaved roads around the sample sites. It is also noted that the mean mass concentration was 2 times lower and higher than that of the dry and wet seasons, respectively.

The higher PM mass concentrations during the dry season are likely due to secondary aerosol formation from photochemical reactions [21, 24] and also due to absence of scavenging by rain droplets. However, an assessment of secondary aerosol formation and the collection, identification, and measurement of secondary aerosols precursor's gases was not done in this study. No clear relationship was observed between the minimum temperature and the measured mass concentration.

Figure 3 shows that all sites except KWWT have $PM_{10}$ mass concentration below the 24-h Ethiopian EPA and WHO guideline value of 150 µg/m$^3$. However, the fact that $PM_{10}$ concentrations approaching 150 µg/m$^3$ at five sites suggest that violation of the 24-h guideline value may also be possible. The result also shows that the annual average $PM_{10}$ guideline value (50 µg/m$^3$) has been violated at several sites. However, the long rainy season (July–September) would significantly lower the $PM_{10}$ concentration, which may help to keep the annual average low. $PM_{10}$ concentrations ranged between 35 and 97 µg/m$^3$, which are lower than what was observed in this study [1]. The difference in results may be due to variation in sampling methodologies. The previous researcher used portable Airmetrics, MiniVol samplers to monitor the concentration of $PM_{10}$ in the ambient air of Addis Ababa.

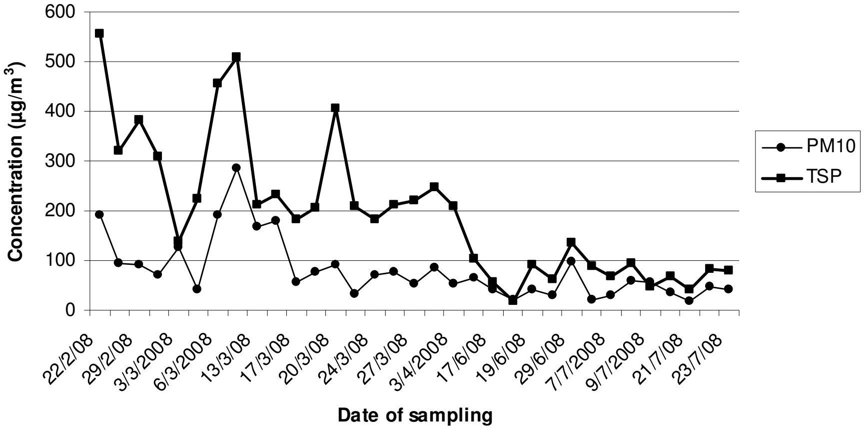

Figure 3. Temporal variations of $PM_{10}$ and TSP (µg/m$^3$).

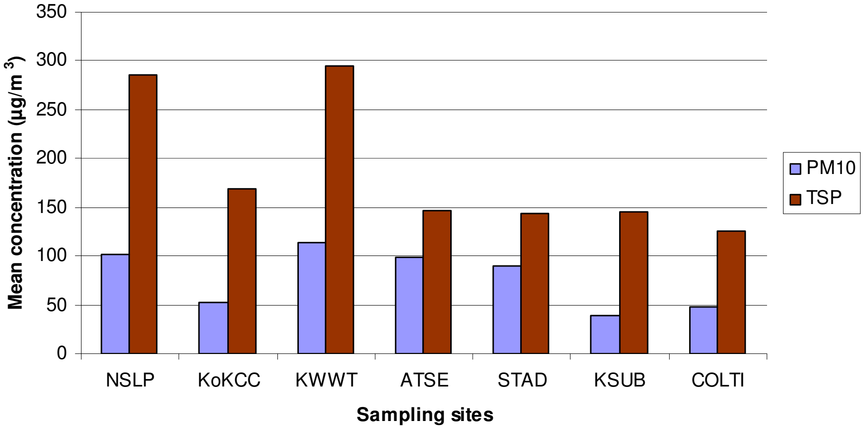

Figure 4. Spatial variations of $PM_{10}$ and TSP (µg/m$^3$).

Comparison of $PM_{10}$ with TSP mass concentration is shown in Figure 4. The $PM_{10}$ to TSP mass ratio was between 0.26 and 0.67. The result shows that $PM_{10}$ contributed approximately 42% to the TSP mass concentration. The remaining portion may be attributed to particulates with an aerodynamic size of greater than 10 micron. The result indicates that both fine and coarse particulates contributed to atmospheric aerosol mass concentration of collected filter mass. Wojas and Almquist found out that $PM_{2.5}$ mass contributed approximately 95% to $PM_{10}$ while > 60% to TSP [24]. Similar studies conducted by other researchers [25] indicated that $PM_{10}$ contributed about 75% of TSP mass. The relatively low contribution of $PM_{10}$ to the TSP indicating that the emission of fine particulates is low as compared to other big cities.

Coarse particles are linked with disease and death. Lippmann *et al.* [26] attempted to identify components of particulate matter and other air pollution mixtures that were associated with excess daily deaths and hospital admissions of the elderly in the Detroit metropolitan area. The researchers reported that deaths from respiratory diseases were associated with $PM_{10}$ and total suspended particulates. They also found that relative risks of the coarse particle fractions were similar to those for $PM_{2.5}$, and even higher in the case of ischemic heart disease and stroke.

### *Elemental composition of $PM_{10}$*

*ICP-AES Analysis*. The average elements concentration of $PM_{10}$ at sampling sites is shown in Table 2. Although analysis of filter samples was made for 22 elements, those elements, which are detected, are indicated in the table. Crustal elements including Al, Ca, Fe, Mg, Na, Zn and K were the predominant species and the concentrations of these elements exceed 1 µg/m$^3$ in most cases.

It is noted that calcium was the most abundant species. The highest and lowest peak value of calcium was 91.1±77.6 and 17.1±13.5 µg/m$^3$, which were observed at KoKKC and STAD sites, respectively. The least abundant crustal species was strontium 0.03±0.01 µg/m$^3$ which was observed at NSLP, KSUB, ATSE and STAD sites. In general the concentration of elements is in the order of Ca > Na > K > Zn > Sb > Al > Mg > B > Fe > Mg. Paved and unpaved road dust is the major sources of Ca, Al, Fe, Mg, Zn, Na, and K.

Table 2 compares trace elements concentration of $PM_{10}$ samples at different sites. The trace metals that were identified include Cr, Ni, Li, Co, Cu, and V. It was observed that Cr is identified at all sampling sites. The highest mean value was 1.06±0.26 µg/m$^3$ (KWWT) and the lowest was 0.297±0.295 µg/m$^3$ (KoKCC). Comparison of the value with a previous study conducted in Bangladesh indicates that, Cr concentration of Addis Ababa is much lower than that of Dhaka (25.2±12.7 µg/m$^3$) and Rajshahi (9.34±5.44 µg/m$^3$) [27]. Co was identified at four sampling sites. The highest mean value was observed at STAD (0.17 µg/m$^3$) and the lowest value was obtained at NSLP site (0.11 µg/m$^3$). Cu was also identified in all sampling sites. The highest and the lowest peak values were 0.11±0.06 µg/m$^3$ (observed at STAD site) and 0.008±0.007 µg/m$^3$ (KSUB site), respectively. The concentration of Cu in ambient air of Addis Ababa is lower than that of Dhaka (13.2±43.4 µg/m$^3$) and Rajshahi (2.58±1.86 µg/m$^3$) [27]. The maximum and minimum concentrations of Li were 0.17±0.02 µg/m$^3$ (STAD site) and 0.02 µg/m$^3$ (NSLP site), respectively. Similarly, the maximum and minimum concentration of B was 2.73±0.62 µg/m$^3$ (NSLP site) and 1.3±1.2 µg/m$^3$ (STAD site), respectively. Mo was identified at KWWT and STAD sites whereas S was identified at STAD site. This result shows that the concentration of Ni in Addis Ababa is far below USEPA air quality guideline value of 25 µg/m$^3$. The highest and lowest peak values of V were 0.02±0.01 µg/m$^3$ (STAD site) and 0.016±0.007 µg/m$^3$ (KoKCC site), respectively. This indicates that the concentration of V in Addis Ababa is far below the US air quality guideline value of 200 µg/m$^3$. The maximum and minimum concentrations of Sb were 12.4.7±0.3 µg/m$^3$ (ATSE site) and 0.03±0.01 µg/m$^3$ (STAD site). Comparison among the sampling sites indicates that STAD site has higher sulfur whereas in other sites trace metals concentration is high. Since the trace metals are typically associated with anthropogenic emissions (traffic, combustion of fossil fuels, various industries), their concentration is expected to be higher at sites with more such activities.

Table 2. Mean elements concentration (μg/m$^3$) of PM$_{10}$ samples.

| Element | Elements concentration (μg/m$^3$) of PM$_{10}$ for different sampling sites | | | | | |
|---|---|---|---|---|---|---|
| | NSLP | KoKCC | KWWT | KSUB | ATSE | STAD |
| Al | 3.03±0.6 | 2.69±1.95 | 3.63± 1.24 | 2.23±0.41 | 2.25±0.48 | 1.14 ±1.12 |
| Ca | 35.1±18.6 | 91.1±77.6 | 35.3±18.9 | 25.7±0.9 | 36.7±23.1 | 17.1±13.5 |
| Cr | 0.77±0.21 | 0.297±0.295 | 1.06±0.26 | 0.9±0.15 | 0.64±0.04 | 0.42±0.29 |
| Co | 0.11±0.02 | ND | 0.13 | ND | 0.14 | 0.17 |
| Cu | 0.07±0.07 | 0.07±0.076 | 0.02±0.00 | 0.008±0.007 | 0.02 | 0.11±0.06 |
| Fe | 1.46±0.42 | 1.33±0.85 | 2.22±0.14 | 0.82±0.25 | 0.95±0.21 | 0.72±0.42 |
| Li | 0.02 | 0.052±0.06 | 0.04± 0.04 | 0.04 | 0.03 | 0.17±0.02 |
| Mg | 1.12±0.46 | 2.4±2.36 | 1.74±0.29 | 0.97± 0.04 | 1.32±0.59 | 0.85±0.48 |
| Mn | 0.1±0.01 | 0.155±0.13 | 0.17±0.02 | 0.05±0.01 | 0.11±0.01 | 0.05±0.02 |
| Sr | 0.03±0.01 | ND | ND | 0.03± 0.00 | 0.04±0.02 | 0.03±0.02 |
| Ti | 0.1±0.03 | 0.077±0.05 | ND | 0.06± 0.04 | 0.07±0.05 | 0.03±0.03 |
| Ni | 0.01 | ND | ND | ND | ND | ND |
| Zn | 7.57±1.76 | 10.41±6.78 | 7.24±2.15 | 5.67±1.21 | 7.13±3.6 | 7.68±6.28 |
| Na | 21.0±2.8 | 28.1±13.8 | 22.5±2.7 | 20.4±2.4 | 21.7±4.7 | 13.6±6.3 |
| K | 7.4±1.07 | 12.3±9.1 | 7.67±1.42 | 6.46±0.63 | 7.4±1.5 | 4.89±2.3 |
| B | 2.73±0.62 | 2.05±1.37 | 2.7±0.87 | 1.82±1.06 | 1.84±0.8 | 1.3±1.2 |
| Sb | ND | 1.297±0.53 | 11.8±0.3 | ND | 12.4±0.3 | 0.03±0.01 |
| V | ND | 0.016±0.007 | ND | ND | ND | 0.02±0.01 |
| Mo | ND | ND | 1.33±0.27 | ND | ND | 1.55±0.63 |
| Cd | ND | ND | ND | ND | ND | 0.02±0.007 |
| S | ND | ND | ND | ND | ND | 10.9±10.1 |

Vegetative burning, residential wood combustion, and cooking are also the sources of K, V, Ni, S, Co and B are associated with emissions from motor vehicles, residual oil combustion and incineration [28]. There is no significant difference in mean Li, Cu, Co, Cr, Mo, V and Ni concentrations between sampling sites, which may indicate that emission sources are spatially distributed. However there is significant difference in B, S and Sb concentration between STAD and other site. This may suggest the existence of specific emission sources, which requires further investigations.

Crustal and trace metals contribute only a very small fraction (0.04-0.32%) of the total PM$_{10}$ mass. The remaining portion may be attributed to organic carbon (OC), elemental carbon (EC), silicon and water-soluble constituent of atmospheric aerosol [28]. Mass concentrations reconstructed from chemical composition indicated that ~35-65% of the PM$_{10}$ mass was due to geologically derived material and ~35-60% was due to OM and EC [1]. Of the crustal and trace metal fraction, the former contributes more than 98% of the total portion. A comprehensive chemical characterization of PM$_{2.5}$ and PM$_{10}$ samples at urban and near rural sites in Switzerland indicated that crustal metals were found to be the predominant species in the coarse fraction [29]. The presence of crustal and trace metals in the present study suggests existence of combination of sources.

Table 3 shows the correlation coefficients of metal species in PM$_{10}$ mass. Although source apportionment is outside the scope of this research, it is noted that crustal elements such as Al with Zn, Ca with Mg and Sr, Mg with Mn and Sr and Zn with Na have strong correlation. Similarly Cr has strong correlation with S as do Cu with B and B with V. It is also clear from the table that Ni has strong correlation with Al, Ca, Cr, Cu, Fe, Li, Mn, Ti, Zn, Na, K, B and Co. Strong correlation between elements may suggest the existence of identical emission sources.

Wojas and Almquist *et al.* reported that metals such as Ca, Co, Cu, Fe, K, Mg, Mn, Mo, Ni, Pb, Sb, Si, and Zn have high correlation coefficients [24].

Table 3. Correlation coefficient for the elements in $PM_{10}$.

| Elem | Al | Ca | Cr | Cu | Mg | Fe | Li | Mn | Sr | Ti | Zn | Na | K | B | S | Sb | Co | Mo | Ni | V |
|---|---|---|---|---|---|---|---|---|---|---|---|---|---|---|---|---|---|---|---|---|
| Al | 1 | -0.25 | 0.04 | -0.02 | 0.09 | 0.13 | -0.06 | 0.03 | 0.01 | 0.03 | 0.93 | -0.28 | 0.33 | -0.26 | -0.11 | -0.15 | 0.28 | -0.33 | 0.88 | -0.9 |
| Ca |  | 1 | -0.22 | 0.33 | 0.95 | 0.1 | -0.24 | 0.75 | 0.98 | 0.13 | 0.78 | 0.78 | 0.32 | -0.42 | -0.91 | 0.08 | 0.83 | -0.59 | 0.83 | -0.49 |
| Cr |  |  | 1 | -0.58 | -0.51 | 0.33 | -0.6 | -0.3 | -0.7 | 0.52 | -0.09 | -0.08 | -0.86 | -0.29 | 0.91 | -0.24 | 0.51 | 0.02 | 0.92 | -0.32 |
| Cu |  |  |  | 1 | 0.02 | -0.05 | 0.77 | -0.1 | 0.21 | -0.29 | -0.32 | -0.39 | 0.79 | 0.82 | -0.45 | -0.48 | 0.13 | -0.33 | -0.88 | 0.67 |
| Mg |  |  |  |  | 1 | 0.44 | -0.05 | 0.87 | 0.88 | 0.14 | 0.77 | 0.76 | 0.24 | -0.45 | -0.92 | -0.03 | 0.09 | 0.26 | 0.3 | -0.55 |
| Fe |  |  |  |  |  | 1 | -0.38 | 0.67 | 0.03 | 0.71 | 0.49 | 0.41 | -0.35 | -0.32 | -0.9 | -0.52 | 0.54 | 0.01 | 0.97 | -0.67 |
| Li |  |  |  |  |  |  | 1 | -0.4 | 0.09 | -0.81 | -0.66 | -0.66 | 0.91 | 0.88 | -0.17 | -0.45 | -0.55 | 0.47 | -0.98 | 0.53 |
| Mn |  |  |  |  |  |  |  | 1 | 0.6 | 0.44 | 0.78 | 0.74 | -0.07 | -0.54 | -0.96 | 0.13 | 0.2 | 0.08 | 0.94 | -0.85 |
| Sr |  |  |  |  |  |  |  |  | 1 | -0.05 | 0.67 | 0.69 | 0.45 | -0.32 | -0.91 | 0.05 | 0.46 | -1 | 0.14 | -0.31 |
| Ti |  |  |  |  |  |  |  |  |  | 1 | 0.65 | 0.58 | -0.72 | -0.59 | -0.21 | 0.08 | 0.87 | -0.6 | 0.95 | -0.83 |
| Zn |  |  |  |  |  |  |  |  |  |  | 1 | 0.98 | -0.32 | -0.83 | -0.63 | 0.26 | 0.63 | -0.52 | 0.92 | -0.91 |
| Na |  |  |  |  |  |  |  |  |  |  |  | 1 | -0.33 | -0.28 | -0.56 | 0.28 | 0.56 | -0.47 | 0.96 | -0.9 |
| K |  |  |  |  |  |  |  |  |  |  |  |  | 1 | 0.08 | -0.61 | -0.23 | -0.53 | 0.27 | -0.99 | 0.19 |
| B |  |  |  |  |  |  |  |  |  |  |  |  |  | 1 | 0.15 | -0.41 | -0.34 | 0.24 | -0.99 | 0.96 |
| S |  |  |  |  |  |  |  |  |  |  |  |  |  |  | 1 | -0.05 | - | - | - | -0.99 |
| Sb |  |  |  |  |  |  |  |  |  |  |  |  |  |  |  | 1 | -0.3 | -0.98 | -1 | -0.32 |
| Co |  |  |  |  |  |  |  |  |  |  |  |  |  |  |  |  | 1 | -0.88 | 0.98 | -0.56 |
| Mo |  |  |  |  |  |  |  |  |  |  |  |  |  |  |  |  |  | 1 | -0.18 | 0.37 |
| Ni |  |  |  |  |  |  |  |  |  |  |  |  |  |  |  |  |  |  | 1 | 0.7 |
| V |  |  |  |  |  |  |  |  |  |  |  |  |  |  |  |  |  |  |  | 1 |

*SEM-EDAX Analysis.* Both size distribution and composition of atmospheric aerosol particulates were derived from the Scanning Electron Microscope Energy Dispersive X-ray Spectroscopy (SEM-EDAX) analyses for $PM_{10}$ samples.

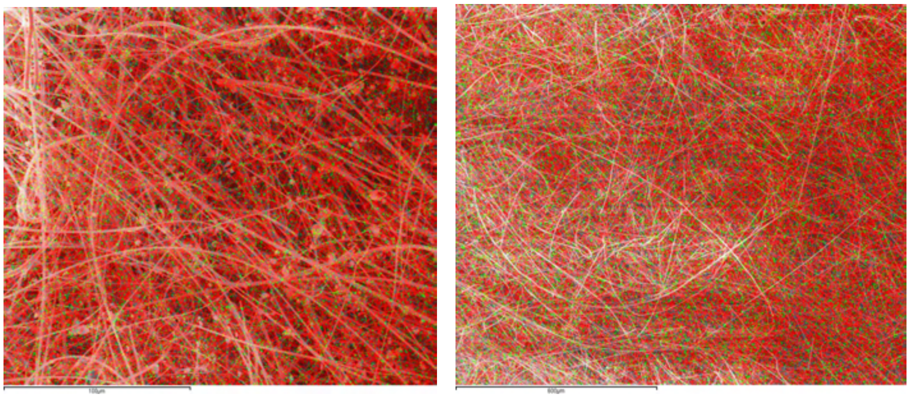

(a) (b)

Figure 5. Distribution of silica (red) and alumina (green) (a) and Distribution of silica (red) and sodium (green) (b).

Table 4. Relative percentage of elements in $PM_{10}$ samples.

| Element | Sampling Site | | | | | |
|---|---|---|---|---|---|---|
| | NSLP | KoKCC | KWWT | KSUB* | ATSE | STAD* |
| Na | 4.97± 0.33 | 5.82±1.04 | 7.37±0.73 | 5.77 | 5.43±0.04 | 5.59 |
| Mg | 0.073±0.06 | 0.205±0.049 | 0.32±0.03 | 0.24 | 0.165±0.0002 | 0.18 |
| Al | 2.02±0.24 | 2.4±0.35 | 3.3±0.4 | 2.26 | 2.09±0.003 | 2.14 |
| Si | 18.3±1.8 | 19.5±3.1 | 27.4±3.2 | 19.8 | 17.8±0.4 | 18.8 |
| Cl | 0.14±0.22 | 0.035±0.048 | ND | 0.11 | 0.085±0.0001 | ND |
| K | 1.78±0.22 | 1.62±0.21 | 2.5±0.28 | 1.76 | 1.69±0.01 | 1.71 |
| Ca | 1.02±0.09 | 1.04±0.12 | 1.52±0.18 | 1.16 | 1.07±0.0004 | 1.15 |
| Zn | 2.59±0.06 | 2.23±0.31 | 3.52±0.37 | 2.49 | 2.69±0.04 | 2.39 |
| Ba | 3.4±0.42 | 2.86±0.17 | 4.6±0.4 | 3.14 | 3.2±0.03 | 3.11 |
| O | 54.9±1.5 | 54.2±2.7 | 46.6±2.7 | 53.6 | 54.9±0.7 | 54.6 |
| Fe | 0.10±0.13 | 0.14±0.01 | 0.17±0.02 | 0.11 | 0.065±0.004 | ND |
| C | 10.7±1.5 | 9.7±2.74 | 2.71±3.8 | 9.41 | 10.8±0.37 | 10.3 |
| Cu | ND | 0.205±0.08 | 0.09±0.13 | 0.11 | ND | ND |

* Shows a single spectrum analysis result.

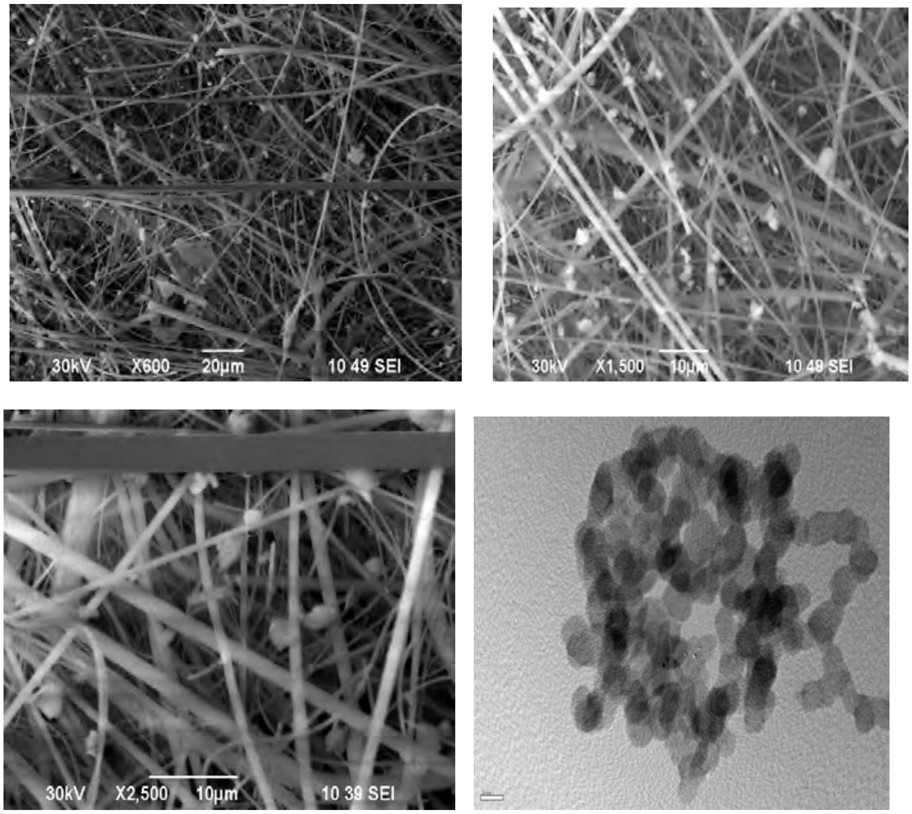

Figure 6. SEM image of size distribution of particulate matter of aerosol samples on the filter.

Representative SEM-EDAX images indicating the relative distribution of elements on the filter samples, silica (red) and alumina (green) and silica (red) and sodium (green) are shown in Figure 5a and 5b, respectively. It can be seen that silica is predominant compared to aluminium and sodium which suggests abundance of alumino-silicate dust particles. Furthermore, result of elemental composition using SEM-EDAX analysis is shown in Table 4. The result also confirms that Si, Al, Na, Zn, Ba, K and C are the predominant species. Crustal materials contributed from 76 to 95% and the contribution of C and Cu was in the range between 5 and 24%. The high proportion of Si, Ca, Na, and K in the filter samples suggests the aerosols are predominately originated from geological sources. The presence of C on the filter samples can possibly be attributed to biomass combustion, fossil fuel combustion, and waste burning activities.

The size distribution of particulates for a representative samples is shown in Figure 6. The size distribution of aerosol particles as derived from SEM analysis for all sampling sites was in 0.43-9.3 µm range and it is also observed that 47% of the particles have an average diameter less than 2.5 micrometer. The SEM micrograph of the filter mass shows that, most of the particles possess spherical and circular shape.

## CONCLUSIONS

The levels of atmospheric aerosols were determined at seven urban and peri-urban sites of Addis Ababa, Ethiopia. The major findings of this study based on samples collected during dry and wet seasons of 2008 showed that the mean TSP concentration of Addis Ababa was 195± 141 $\mu g/m^3$. The highest and lowest values were 556 $\mu g/m^3$ (Feb. 2008 at NSLP site) and 17 $\mu g/m^3$ (June 2008 at KSUB), respectively. The mean TSP value surpassed the lower limit of WHO safe guideline value of 150-230 $\mu g/m^3$ [30]. The mean $PM_{10}$ mass of Addis Ababa was 80±61 $\mu g/m^3$. The maximum and minimum values were 285 $\mu g/m^3$ (Feb. 2008 at KWWT) and 17 $\mu g/m^3$ (July 2000 at COLTI), respectively. 79% of the $PM_{10}$ values were below the 24-h Ethiopian EPA and WHO guideline values. The mean values of $PM_{10}$ of Addis Ababa were found to be higher than that reported for most European cities. The mean PM10 to TSP mass ratio was in the range of 0.26 to 0.67 and the $PM_{10}$ mass contributed about 42% of the TSP mass. The remaining portion may be attributed to fine particulates. ICP analysis of $PM_{10}$ samples showed that Al, B, Ca, Cd, Co, Cr, Cu, Fe, K, Li, Mg, Mn, Mo, Na, Ni, S, Sb, Sr, Ti, V and Zn were identified. The average element concentration order was Ca > Na > K > Zn > Sb > B > Al > V > Mg > S > Fe. These elements contributed about 0.1% of the $PM_{10}$ mass. The elements concentrations were far lower than those found in urban areas of Europe and Asia. SEM-EDAX analysis showed that Si, Al, Na, Zn, Ba, K and C were the predominant components of the $PM_{10}$ fractions. The analysis results revealed that, 76-95% was of geological origin. The remaining 5-24% was carbon compounds and small amount of Cu. The presence of carbon in the samples may be due to incomplete combustion of fossil fuels and biomass around the sampling sites. The size distribution of aerosol particles from SEM analysis was in 0.43-9.3 µm ranges. While the present work provides an insight regarding the level of TSP and $PM_{10}$ mass concentration and their composition in Addis Ababa, further studies will be needed to characterize $PM_{10}$ and $PM_{2.5}$ (including ionic species, EC, OC and VOCs) with more sampling coverage. In addition, meteorological conditions such as wind speed, wind direction, precipitation and relative humidity need to be determined on continuous basis.

## REFERENCES

1. Etyemezian, V.; Tesfaye, M.; Yimer, A.; Chow, J.C.; Mesfin, D.; Nega, T.; Nikolich, G.; Watson, J.G.; Wondmagegn, M. *Atmos. Environ*. 2005, 39, 7849.
2. Central Statistics Authority of Ethiopia (CSA) *Population and housing census of Ethiopia*, *Statistical Abstract*, **1994**.

3. Kume, A. *Ph.D. Thesis*, Addis Ababa University, Ethiopia, **2009**.
4. De Koning, H.W.; Kretzschmar, J.G.; Akland, G.G.; Bennett, B.G. *Atmos. Environ*. **1986**, 20, 101.
5. Dockery, D.W.; Pope III, C.A.; Xu, X.; Spengler, J.D.; Ware, J.H.; Fay, M.E.; Ferris Jr., B.G.; Speizer, F.E. *New England J. Med*. **1993**, 329, 1753.
6. Reichhardt, T. *Environ. Sci. Technol.* 1995, 29, 360.
7. Pope III, C.A.; Dockery, D.W.; Schwartz, J. *Inhalation Toxicology* **1995**, 7, 1.
8. Pope, C.A.; Dockery, D.W. *J. Air Waste Manage. Assoc.* **2006**, 56, 709.
9. Pope, C.A.; Burnett, R.T.; Thurston, G.D.; Thun, M.J.; Calle, E.E.; Krewski, D.; Godleski, J.J. *Circulation* **2004**, 109, 71.
10. Pope, C.; Burnet, R.; Thun, M.J.; Calle, E.E.; Krewski, D.; Ito, K.; Thurston, G.D. *J. Am. Med. Assoc.* **2002**, 287, 1132.
11. Dockery, D.W.; Stone, P.H. *New England J. Med*. **2007**, 356, 511.
12. Donaldson, K.; MacNee, W. *Intern. Hygiene Environ. Health* **2001**, 203, 411.
13. IPCC in *Climate Change*, Houghton, J.T.; Ding, Y.; Griggs, D.J.; Noguer, M.; van der Linden, P.J.; Dai, X.; Maskell, K.; Johnson, C.A. (Eds.), Cambridge University Press: Cambridge, UK; **2001**.
14. Morawska, L.; Thomas, S.; Bofinger, N.; Wainwright, D.; Neale, D. *Atmos. Environ.* **1998**, 32, 2467.
15. Weisel, C.P. *Environ. Health Perspect* **2002**, 110 (suppl 4), 527.
16. Zhou, W.; Yuan, D.; Ye, S.; Qi, P.; Fu, C.; Christiani, D.C. *Int. J. Occup. Environ. Health* **2001**, 7, 23.
17. Harris, S.J.; Maricq, M.M. *J. Aerosol Sci.* **2001**, 32, 749.
18. Guo, Y.L.; Lin, Y.C.; Sung, F.C.; Huang, S.L.; Ko, Y.C.; Lai, J.S.; Su, H.J.; Shaw, C.K.; Lin, R.S.; Dockery, D.W. *Environ. Health Prospect* **1999**, 10, 1001.
19. Artinano, B.; Salvator, P.; Alonso, D.G.; Querol, X.; Alastuey, A. *Environ. Poll.* **2003**, 125, 453.
20. Tsai, Y.I.; Cheng, M.T. *Chemosphere* **2004**, 54, 1171.
21. Drewnick, F.; Schwab, J.J.; Jayne, J.T.; Canagaratna, M.; Worsnop, D.R.; Demerjian, K.L.; *Aerosol Sci. Technol.* **2004**, 38, 92.
22. Rodrı´guez, S.; Van Dingenen, R.; Putaud, J.P.; Dell'Acqua, A.; Pey, J.; Querol, X.; Alastuey, A.; Chenery, S.; Ho, K.F.; Harrison, R.; Tardivo, R.; Scarnato, B.; Gemelli, V. *Atmos. Chem. Phys.* **2007**, 7, 2217.
23. Ghermandi, G.; Laj, P.; Capotosto, M.; Cecchi,R.; Riontino, C. *Nuclear Instruments and Methods in Physics Research B* **1999**, 150, 392.
24. Wojas, B.; Almquist, C. *Atmos. Environ.* **2007**, 41, 9064.
25. Yusoff, M., Rashid, M., *Symposium of Malaysian Chemical Engineers*, Kuala Lumpur, Malaysia; **1987**; pp 1-16.
26. Lippmann, M.; Ito, K.; Nádas, A.; Burnett, R.T. *Health Effects Institute Research Report Number 95*, 2000.
27. Begum, B.A.; Kim, E.; Biswas, S.K.; Hopke, P.K. *Atmos. Environ.* **2004**, 38, 3025.
28. Watson, J.G.; Chow, J.C.; Rogers, C.F.; DuBois, D.; Cahill, C. *Report, prepared for the California Regional Particulate Air Quality Study*, California Air Resources Board, Sacramento, Desert Research Institute, **1997**.
29. Hueglina, C.; Gehriga, R.; Baltenspergerb, U.; Gyselc, M.; Monnd, C.; Vonmonta, H. *Atmos. Environ.* **2005**, 39, 637.
30. World Health Organization *Ambient Air Quality Guideline*, World Health Organization: Geneva; **2005**.